Molecular dynamics simulations: Development and Applications

Vom Fachbereich Chemie

der Technischen Universität Darmstadt

zur Erlangung des akademischen Grades eines

Doctor rerum naturalium (Dr. rer. nat.)

genehmigte

Dissertation

eingereicht von

Dipl.-Ing. Konstantin B. Tarmyshov

aus Tyup, Kirgisien

Berichterstatter:	Professor Dr. Florian Müller-Plathe
Mitberichterstatter:	Professor Dr. Rolf Schäfer
Tag der Einreichung:	2006-12-19
Tag der Mündlichen Prüfung:	2007-02-05

Darmstadt 2006

D17

Acknowledgements

First of all, I would like to thank Prof. Florian Müller-Plathe for giving me the great opportunity to work in his group and to profit enormously from his exceptional scientific knowledge. I am also very grateful to him for his kind guidance in both research and life, which allowed me to develop my professional skills and personality immensely. Thanks to his sense of humor and inspiration, the years of my PhD work turned into a very pleasant time.

Many thanks to all of my colleagues for fine and warm working atmosphere that they created. Obrigado to Welchy Cavalcanti for all the funny times and especially for help while getting settled down in Darmstadt. I am grateful to Daniel dos Santos for his support and help with SuSE Linux and helpful scientific discussions. I am very thankful to Volker Weiß for his patience while explaining me that part of physical chemistry that physicists in Russia do not learn. Big thanks to Meimei Zhang for her help with finalizing this thesis. I am grateful to Sudip Roy for sharing with me his experience in quantum calculations. I wish to thank Thomas Müller who shared with me the administration of our IT facilities. I also appreciate scientific support and sense of humor of Hossein Eslami. Special thanks to Gabriele General for her help with organizational and "Life in Germany" issues.

I want to thank all of my friends for their support.

I thank my family for who I am now.

Table of contents

List of figures

List of tables

Zusammenfassung

Molekulare Computersimulationen sind in der Lage, ein detailliertes Bild eines chemischen, physikalischen oder biologischen Prozesses zu liefern. Diese Technik wurde in den letzten 50 Jahren entwickelt und wird heutzutage bei der Bearbeitung einer Vielzahl von Problemen in vielen unterschiedlichen Wissenschaftsfeldern eingesetzt. Insbesondere sind quantenchemische Berechnungen zum Studium kleiner Systeme mit großer Genauigkeit einsetzbar, wenn die Elektronenstruktur der Moleküle eine Rolle spielt. Molekulardynamische Computersimulationen werden benutzt, um die örtliche und zeitliche Entwicklung eines molekularen Systems zu untersuchen. Kapitel 1 gibt einen kurzen Überblick der Methoden, die derzeit im Bereich der molekularen Simulationen genutzt werden, beschreibt ihre Grenzen und ihre Entwicklung.

Kapitel 2 beschreibt die Methoden, die in dieser Arbeit zum Einsatz kamen. Kapitel 3 behandelt mögliche Anwendungsbereiche der untersuchten Systeme.

Genauso wichtig wie die wissenschaftliche Erforschung von Methoden und Algorithmen in der Molekulardynamik ist die Weiterentwicklung der Werkzeuge. In Kapitel 4 wird eine Strategie zur Parallelisierung des Molekulardynamikprogramms YASP für shared-memory Computerarchitekturen beschrieben. Die Parallelisierung wurde auf die rechenintensiven Teile beschränkt: Konstruktion der Nachbarliste, Berechnung der nichtbindenden, Winkel- und Diederkräfte und Zwangsbedingungen. Der größte Teil des seriellen FORTRAN-Codes wurde erhalten. Parallele Konstrukte wurden unter Einsatz des OpenMP-Standards als Compilerdirektiven eingefügt. Nur im Fall der Nachbarliste mußte die Datenstruktur geändert werden. Der parallele Code erreicht eine zufriedenstellende Beschleunigung gegenüger der seriellen Version für Systeme aus einigen tausend Atomen und mehr. Auf einer IBM Regatta p690+ steigt der Durchsatz mit der Anzahl der Prozessoren bis zu einem Maximum von 12 – 16 Prozessoren abhängig von der Charakteristik des simulierten Systems. Auf Zweiprozessor-Xeon-Systemen beträgt die Beschleunigung bis zu 1.7. Sicherlich sind diese Ergebnisse von großem Interesse für andere Arbeitsgruppen in Forschung und Industrie, die ihre eigenen Simulationscodes optimieren wollen.

Um einen molekularen Rezeptor zu entwickeln oder aus einer Auswahl bereits bekannter Rezeptoren einen für die jeweilige Anwendung geeigneten Rezeptor auszuwählen, bedarf es einer genauen Kenntnis der nichtkovalenten Wechselwirkung zwischen dem Rezeptor und dem Gastmolekül. Zusätzlich möchte man Einfluss auf den Assoziations- bzw. Dissoziationsprozess durch Veränderung äußerer Parameter (pH, Salzkonzentration usw.) nehmen können. Kapitel 5 ist den Molekulardynamiksimulationen gewidmet, die durchgeführt wurden, um die mikroskopische Struktur und die Dynamik des Bindens von Kationen an Cucurbit[6]uril (CB[6]) in reinem Wasser und in wässrigen Lösungen von Natrium-, Kalium- bzw. Kalziumchlorid zu untersuchen. Die Molaritäten der Lösungen waren jeweils 0.183M für die Salze und 0.0184M für CB[6]. Die Kationen binden ausschließlich an die Carbonyl-Sauerstoffatome des CB[6]. Sie gelangen nicht in das Innere des CB[6]-Moleküls. Komplexe mit Na^+- oder K^+-Ionen enthalten meist nur ein Kation, während für Ca^{2+}-Ionen in etwa gleichem Maße Komplexe mit ein oder zwei Kationen beobachtet werden.

Die Bindungsdynamik hängt stark von der Art des Kations ab. Geringe Größe und hohe Ladung des Kations führen zu einer längeren Verweildauer des Ions an einem bestimmten Carbonyl-Sauerstoffatom. Die Dynamik der Diffusion entspricht der jeweiligen Bindungsstärke (Affinität) des Kations: Je stärker die Bindung, desto langsamer die Diffusion und die Reorientierungsdynamik. Nach der Bindung an das CB[6]-Molekül wandern Natrium- und Kaliumionen meist von einem Carbonyl-Sauerstoffatom zum benachbarten oder zum übernächsten Sauerstoffatom. Kalziumionen hingegen zeigen keine solche Wanderung. Sie sind vorwiegend an nur ein Sauerstoffatom gebunden. Der Innenraum des CB[6]-Moleküls, der durch die beiden Ebenen, die durch die Sauerstoffatome gebildet werden, begrenzt ist, nimmt nur wenige (null bis vier) Wassermoleküle auf. Die Verweildauer der Wassermoleküle im Innenraum wird durch Natrium- und Kaliumionen kaum beeinflußt. Das in der Literatur vorgeschlagene Modell, gemäß dem die Ionen eine Art Deckel über den Portalen des CB[6]-Innenraumes bilden, kann demnach nicht bestätigt werden. Die Verlangsamung des Wasseraustausches zwischen dem Innenraum und der Lösung ist eine Folge der generell langsameren Dynamik in Gegenwart von Salz und der Stabilität der Hydrathülle der Ionen. Eine Studie des Bindungsverhaltens von einfachen hydrophoben (Lennard-Jones) Molekülen an CB[6] zeigt, dass diese Teilchen nicht nennenswert an CB[6] binden. Durch Variation der Größe der hydrophoben Teilchen wurde gezeigt, dass dieser Parameter für eine stabile Komplexbildung entscheidend ist.

Ein weiteres Gebiet dieser Arbeit beschäftigt sich mit Grenzschichten zwischen metallischen Oberflächen und organischen Substraten. Vor allem für Übergangsmetalle ist es anspruchsvoll, Wechselwirkung zu beschreiben, da die Übergangsmetalle mit einer großen Anzahl von organischen Substanzen chemische Bindungen unterschiedlicher Stärke ausbilden. In Kapitel 6 wird die Adsorption von Isopropanol auf einer Platin(111)-(Pt(111))-Oberfläche unter untersättigter und übersättigter Bedeckung mit Molekulardynamiksimulationen untersucht, wofür auch ein Parametrisierungverfahren entwickelt wurde. Ebenso wurden statische und dynamische Eigenschaften der Grenzschicht zwischen Pt(111) und flüssigem Isopropanol erforscht. Es wird gezeigt, dass untersättigter Bedeckung die Adsorptionsenergie mit der Bedeckung zunimmt. Bei übersättigter Bedeckung (Mehrschichtadsorption) ist die Adsorptionsenergie generell kleiner. Dies stimmt mit Temperatur-programmierten Desorptionsexperimenten überein. Die Analyse der Dichte zeigt eine Anreicherung der Moleküle auf der Oberfläche und darüber eine Verarmung der Moleküle. Die Oszillationen von Anreicherungen und Verarmungen im Dichteprofil sind bis zu einem Abstand von 3 nm von der Oberfläche beobachtbar. Ausserdem zeigt die Verteilung der einzelnen Atomtypen, dass die erste Schicht absorbierter Moleküle eine hydrophobe „Bürste“ von Methylgruppen ausbildet. Diese „Bürste“ bestimmt dann die weiter von der Oberfläche entfernten Verteilungen. In der zweiten Schicht liegen die Methyl- und Methin-Gruppen näher an der Metalloberfläche und die Hydroxylgruppen etwas weiter weg, während in der dritten Schicht die Atomgruppen exakt die umgekehrte Verteilung aufweisen. Dieses abwechselnde Muster wiederholt sich bis zu einer Distanz von 2 nm von der Metalloberfläche. Die Ausrichtung der Moleküle als Funktion von deren Distanz zur Oberfläche wird nur durch die Atomverteilung bestimmt und hängt überraschenderweise nicht von den elektrostatischen oder chemischen Wechselwirkungen von Isopropanol mit der Metalloberfläche ab. Dennoch wird die Bildung von Wasserstoffbrücken in der ersten

Schicht merklich durch diese Wechselwirkungen beeinflusst. Die Wechselwirkungen zwischen Oberfläche und Adsorbat haben nur in der ersten Schicht einen Einfluss auf die Beweglichkeit von Isopropanolmolekülen. In allen weiter enfernten Schichten ist die Beweglichkeit davon unabhängig.

Im Kapitel 7 werden die Hauptaussagen dieser Doktorarbeit zusammengefasst und Perspektiven für die zukünftige Forschung auf diesem Gebiet skizziert.

Summary

Molecular simulations can provide a detailed picture of a desired chemical, physical, or biological process. It has been developed over last 50 years and is being used now to solve a large variety of problems in many different fields. In particular, quantum calculations are very helpful to study small systems at a high resolution where electronic structure of compounds is accounted for. Molecular dynamics simulations, in turn, are employed to study development of a certain molecular ensemble via its development in time and space. Chapter 1 gives a short overview of techniques used today in molecular simulations field, their limitations, and their development.

Chapter 2 concentrates on the description of methods used in this work to perform molecular dynamics simulations of cucurbit[6]uril in aqueous and salt solutions as well as metal-isopropanol interface. This is followed by Chapter 3 that outlines main areas in our life where these systems can be used.

The development of instruments is as important as the scientific part of molecular simulations like methods and algorithms. Parallelization procedure of the atomistic molecular dynamics program YASP for shared-memory computer architectures is described in Chapter 4. Parallelization was restricted to the most CPU-time consuming parts: neighbour-list construction, calculation of non-bonded, angle and dihedral forces, and constraints. Most of the sequential FORTRAN code was kept; parallel constructs were inserted as compiler directives using the OpenMP standard. Only in the case of the neighbour list the data structure had to be changed. The parallel code achieves a useful speed-up over the sequential version for systems of several thousand atoms and above. On an IBM Regatta p690+, the throughput increases with the number of processors up to a maximum of 12-16 processors depending on characteristics of the simulated systems. On dual-processor Xeon systems, the speed-up is about 1.7. Certainly, these results will be of interest to other scientific groups in academia and industry that would like to improve their own simulation codes.

In order to develop a molecular receptor or choose from already existing ones that fits certain needs one must have quite good knowledge of non-covalent host-guest interactions. One also wants to have control over the capture/release process via environment of the receptor (pH, salt concentration, etc.). Chapter 5 is devoted to molecular dynamics simulations preformed to study the microscopic structure and dynamics of cations bound to cucurbit[6]uril (CB[6]) in water and in aqueous solutions of sodium, potassium, and calcium chloride. The molarities are 0.183M for the salts, and 0.0184M for CB[6]. The cations bind only to CB[6] carbonyl oxygens. They are never found inside the CB[6] cavity. Complexes with Na^+ and K^+ mostly involve one cation, whereas with Ca^{2+} single- and double-cation complexes are formed in similar proportions. The binding dynamics strongly depends on the type of cation. A smaller size or higher charge increases the residence time of a cation at a given carbonyl oxygen. The diffusion dynamics also corresponds to the binding strength of cations: the stronger binding the slower diffusion and reorientation dynamics. When bound to CB[6], sodium and potassium cations jump mainly between nearest or second-nearest neighbours. Calcium shows no hopping dynamics. It is coordinated predominantly by one CB[6]

oxygen. A few water molecules (zero to four) can occupy the CB[6] cavity, which is delimited by the CB[6] oxygen faces. Their residence time is hardly influenced by sodium and potassium ions. In the case of calcium the residence time of the inner water increases notably. A simple structural model for the cations acting as "lids" over the CB[6] portal cannot, however, be confirmed. The slowing of the water exchange by the ions is a consequence of the generally slower dynamics in their presence and of their stable solvation shells. The study of binding behaviour of simple hydrophobic (Lennard-Jones) particles by CB[6] showed that these particles do not bind. A simple test showed that the size of hydrophobic particles in this case is important for a stable encapsulation.

Another challenging field of research is the metal-organic interfaces. Particularly, transition metals are more difficult as they form chemical bonds, though sometimes very weak, with a large number of organic compounds. In Chapter 6 a molecular dynamics model and its parameterization procedure are devised and used to study adsorption of isopropanol on platinum(111) (Pt(111)) surface in unsaturated and oversaturated coverages regimes. Static and dynamic properties of the interface between Pt(111) and liquid isopropanol are also investigated. The magnitude of the adsorption energy at unsaturated level increases at higher coverages. At the oversaturated coverage (multilayer adsorption) the adsorption energy reduces, which coincides with findings by Panja *et al.* in their temperature-programmed desorption experiment (ref. 25). The density analysis showed a strong packing of molecules at the interface followed by a depletion layer and then by an oscillating density profile up to 3 nm. The distribution of individual atom types showed that the first adsorbed layer forms a hydrophobic methyl "brush". This "brush" then determines the distributions further from the surface. In the second layer methyl and methine groups are closer to the surface and are followed by the hydroxyl groups; the third layer has exactly the inverted distribution. The alternating pattern extends up to about 2 nm from the surface. The orientational structure of molecules as a function of distance of molecules is determined by the atoms distribution and surprisingly does not depend on the electrostatic or chemical interactions of isopropanol with the metal surface. However, possible formation of hydrogen bonds in the first layer is notably influenced by these interactions. The surface-adsorbate interactions influence mobility of isopropanol molecules only in the first layer. Mobility in the higher layers is independent of these interactions.

Finally, Chapter 7 summarizes main conclusions of the studies presented in this thesis and outlines perspectives of the future research.

1. Introduction: molecular simulation as a scientific instrument

By assuming that everything in our world is built of atoms, we try to picture a molecular process in terms of atoms' movements, mutual interactions, and assemblies, which these atoms produce, like molecules or higher order molecular structures. In order to characterize and understand a certain molecular process, one needs high resolution experimental techniques as well as a model or theory that is able to explain the results or some details of the experiment. Such processes can be, for instance, host-guest encapsulation/release event, possible paths of a chemical reaction, diffusion of small gas or liquid molecules in bulk polymer, structure and diffusion of liquid or polymer melt at the interface with solid surface. Unfortunately, due to the physical and (not least) economical reasons, the experimental instruments can not increase the resolution of the obtained data in space and time without limit. This limitation makes investigation of some processes either very difficult or impossible at all (e.g. measurement of torsional barrier of a molecule or the dynamics of metal cations at the portal of cucurbit[6]uril in aqueous solutions).

Alternatively, if properties of molecular substances need to be predicted, one can use a theory that provides an approximate description of that material. These approximations are inescapable, as there are only few model systems for which the equilibrium properties can be computed exactly (e.g. ideal gas, harmonic crystal). Their relevance to the real world is obviously limited. The properties of each substance are the outcome of the intermolecular interactions, which these theories are based on. Unfortunately, the knowledge of intermolecular interactions is quite limited. This leads to a problem if one tries to validate a particular theory by comparing directly to experiment. That is, if theory and experiment disagree, it may mean that the theory is wrong, or that the estimate of intermolecular interactions is wrong, or both.

In these situations, computer simulations can help to investigate a molecular (physical, chemical, or biological) process. Molecular simulations undergo the same problems in applicability and estimation of intermolecular interactions as any theory. However, here one concentrates on the estimation of interatomic (intermolecular) interactions as precise as possible. The evolution of a system of particles (atoms or electrons) can be monitored then with time by applying Newton's equation of motion and/or the time dependent Schrödinger equation. Properties are then estimated via analyzing the motion of the atoms in the system. Here, one can compare the result of a simulation of a given model system with the predictions of an approximate analytical theory applied to the same model. If now theory and simulations disagree, it means (most of times) that the theory needs improvement. Thus, in this case, the computer simulation becomes the experiment designed to test the theory. Chapter 2 of this work contains more details on how intermolecular interactions are accounted for in atomistic molecular dynamics (MD).

Ideally, a simulation should be as close to reality as possible. That is, a model should be as accurate as possible to describe correctly the properties and behaviour of the system, the size of the system should be large enough to avoid any finite-size effects in

the dynamics of the system, and the simulation time should be long enough to sample relevant processes on a realistic time scale. However, in reality, even with today's computer power, one cannot fulfill all these requirements simultaneously. Therefore, a model chosen to simulate a certain system is often a compromise between computational cost and accuracy.

In the early 1950s the computers became available for nonmilitary use and that was the beginning of the field of computer simulation. With time they prove to be wide applicable, in particular MD simulations (Chapter 3), to interpreting and explaining experimental data or to testing analytical theories. This, in turn, has made the instrument quite spread and has facilitated development of the tool for over half a century since the introduction of the method. The evolution has involved changes in both technical (hardware and software) and scientific (theory and algorithms) sides of the simulations. Along with the development of computers and the software to run on them (operating systems, programming languages, corresponding compilers and optimizers), scientists were obtaining modern instruments to build and improve the performance and analysis of MD simulations. One of the very important developments in computers, which has allowed scientists to speed up their large calculations, was parallel computing. However, by the time when machines and instruments for developing and performing parallel MD simulations became available many sequential programs had been already created. These, obviously, needed to be parallelized.

Today, there are two classes of implementation of parallel MD. The first one is the so-called "shared memory" approach. Molecular dynamics programs that employ this technique are run on a single computer with several processors, which share the same physical memory. The other is the "distributed memory" approach, where MD calculations are distributed over many processors, where each has its own memory. These are usually computers with one ore more processors connected into a network. The upgrade of an MD program using the "shared memory" approach is notably easier compared to the "distributed memory" method. Chapter 4 is devoted to parallelization of a particular MD code (YASP) using the standard "shared memory" approach – OpenMP. The YASP[1-3] code employs classical algorithms that are widely known and employed in the field of MD simulations and can be found in many books (e.g. Allen and Tildesley[4] or Frenkel and Smit[5]). This makes the description of the parallelization strategy useful for other scientists, who want to do the same with their own MD simulation codes.

The scientific (theoretical physical and chemical) component of the MD simulations has been developed as well. At the moment, there is a set of instruments of theory (model), force-field parameterization, and simulation procedures that are quite settled. These are atomistic molecular dynamics simulations. In the model, all interatomic interactions are accounted for via dispersive attraction, repulsion due to the Pauli principle, and electrostatic interactions between partially charged atoms as well as terms describing chemical bonds. The application of the MD simulations to the field of molecular recognition is described in Chapter 5.

Currently, many of new problems cannot be solved by means of the classical MD simulations (e.g. proton transfer in water[6-8] or fuel-cell catalysts and membranes[9]). There is one particularly difficult area for MD simulations – interfaces of metal surfaces, especially transition metals, with organic materials such as polymers. Generally, all metals have the ability to carry electrical currents and to screen external electrical fields.

Moreover, the transition metals have partially filled *d* states, which makes them "greedy" towards electrons of other molecules. As a result of this, clusters and surfaces of these metals often form chemical bonds with other atoms or molecules (chemisorption). The formation of chemical bonds between two molecular assemblies (molecules, clusters, surfaces, and etc.) depends on the electronic configuration. The electronic configuration has a certain spatial distribution, which clearly predefines the mutual orientation of entities bound chemically to each other. In simulations, additional terms are required in classical atomistic MD to account for chemical bonds and mutual position and orientation between the metal assemblies and other atoms or molecules. The standard bonded and non-bonded potentials (Chapter 2) are not capable of simulating the formation and breaking of chemical bonds. Therefore, additional force-field terms are needed to describe the formation of weak chemical bonds between surface and adsorbed molecules. In most investigations the additional potentials are parameterized only approximately and lack a clear parameterization procedure, which could be transferred to different systems. This is especially true for the area of transition metal surfaces and interfaces. Chapter 6 provides more details on the subject and can be considered as an attempt to systematically build a model of metal surfaces, which is applicable for various systems. The interface between platinum (111) surface and 2-propanol (isopropanol) was studied as a test system. Additionally, section 2.2 contains more technical information about the treatment of the electrostatic response of a metal surface to an external field.

Finally, Chapter 7 closes this thesis with an outlook of the future development of molecular dynamics simulations and their impact on the everyday life.

References

(1) Müller-Plathe, F. *Comput. Phys. Commun.* 1993, *78*, 77.
(2) Müller-Plathe, F.; Brown, D. *Comput. Phys. Commun.* 1991, *64*, 7.
(3) Müller-Plathe, F. *Comput. Phys. Commun.* 1990, *61*, 285.
(4) Allen, M. P.; Tildesley, D. J. *Computer Simulation of Liquids*; Oxford University Press: Oxford, 1987.
(5) Frenkel, D.; Smit, B. *Understanding Molecular Simulation: From Algorithms to Applications*, 2nd ed.; Academic Press: San Diego, 2002.
(6) Schmitt, U. W.; Voth, G. A. *J. Phys. Chem. B* 1998, *102*, 5547.
(7) Schmitt, U. W.; Voth, G. A. *J. Chem. Phys.* 1999, *111*, 9361.
(8) Braun-Sand, S.; Strajbl, M.; Warshel, A. *Biophys. J.* 2004, *87*, 2221.
(9) Goddard, W.; Merinov, B.; van Duin, A.; Jacob, T.; Blanco, M.; Molinero, V.; Jang, S. S.; Jang, Y. H. *Mol. Simul.* 2006, *32*, 251.

2. Molecular dynamics simulations

2.1. Classical simulations: atomistic models and force-fields

Classical atomistic molecular dynamics (MD) simulations are a well established set of theory and tools[1,2]. They have proven to be useful for simulations of a very broad range of materials (gases, liquids, polymer melts and crystals, proteins[3], etc.).

These methods treat the atoms of the system as spherical particles with certain masses and describe their dynamics via Newton's equation of motion. The interactions between atoms are described by two types of potential energy terms: bonded and non-bonded. The bonded potential energy terms account for the interactions between atoms that are connected to each other chemically and these are bonds (two atoms), bond angles (three atoms), improper (harmonic) dihedral angles, and torsional dihedral angles (four atoms). The improper dihedral angles are used to keep four atoms in a desired configuration. The non-bonded terms describe pair-wise van-der-Waals attraction, short-range repulsion, and electrostatic interactions.

$$\begin{aligned} V(\mathrm{r},s) &= V_{bonded}(\mathrm{r},s) + V_{non\text{–}bonded}(\mathrm{r},s) \\ &= V_{bond}(\mathrm{r},s) + V_{angle}(\mathrm{r},s) + V_{improper}(\mathrm{r},s) + V_{torsion}(\mathrm{r},s) \\ &+ V_{LJ}(\mathrm{r},s) + V_{electrostatic}(\mathrm{r},s) \end{aligned}$$

where r denotes a set of atomic coordinates and s the force-field parameters. It should be noted that the concrete mathematical form may vary for different implementations. In this thesis only the forms used in the YASP MD code[4-6] will be given. The bond-length interaction function contains two parameters – equilibrium bond length b_0 and the force constant k_b.

$$V_{bond}(\mathrm{r},s) = V_{bond}(b,b_0,k_b) = \sum_{n=1}^{N_b} \frac{1}{2} k_{b,n} \left(b_n - b_{0n}\right)^2$$

The bond-angle term has as the parameters the equilibrium angle φ_0 and the force constant k_φ that can be used in the two following forms.

$$V_{angle}(\mathrm{r},s) = V_{angle}(\varphi,\varphi_0,k_\varphi) = \sum_{n=1}^{N_\varphi} \frac{1}{2} k_{\varphi,n} \left(\varphi_n - \varphi_{n0}\right)^2$$

or

$$V_{angle}(\mathrm{r},s) = V_{angle}(\varphi,\varphi_0,k_\varphi) = \sum_{n=1}^{N_\varphi} \frac{1}{2} k_{\varphi,n} \left(\cos\varphi_n - \cos\varphi_{n0}\right)^2$$

The improper (harmonic) dihedral angles utilize the equilibrium angle θ_0 and the force constant k_θ in the form as following.

$$V_{improper}(\mathrm{r},s) = V_{improper}(\mathrm{r},\theta_0,k_\theta) = \sum_{n=1}^{N_\theta} \frac{1}{2} k_{\theta,n} \left(\theta_n - \theta_{0n}\right)^2$$

The last bonded energy term – dihedral or torsion angles – includes three parameters: the periodicity of the potential p, the equilibrium dihedral angle τ_0, and again a force constant k_τ.

$$V_{torsion}(\mathrm{r},s) = V_{torsion}(\tau,p,\tau_0,k_\tau) = \sum_{n=1}^{N_\tau} \frac{1}{2} k_{\tau,n} \left(1 - \cos[p(\tau_n - \tau_{0n})]\right)$$

The non-bonded interactions are described by the pair-wise dispersive attraction (van-der-Waals), the repulsion at very short distances (Pauli principle), and the Coulomb term. The dispersive attraction and the repulsion are contracted mathematically into one potential energy form, the Lennard-Jones potential. This form is based on two parameters: the inter-atomic interaction energy ε and the atomic excluded volume diameter σ.

$$V_{LJ}(\mathrm{r},s) = V_{LJ}(\mathrm{r},\varepsilon,\sigma) = \sum_{i,j} 4\varepsilon_{ij} \left[\left(\frac{\sigma_{ij}}{r_{ij}} \right)^{12} - \left(\frac{\sigma_{ij}}{r_{ij}} \right)^{6} \right]$$

Ideally, these parameters should be given for each couple of atoms i and j in the system. However, for the sake of simplification, a combination rule is applied. Each atom in the system has its own values of ε and σ, and the parameters for an unlike couple of atoms i and j are derived as follows.

$$\varepsilon_{ij} = \sqrt{\varepsilon_i \varepsilon_j}$$
$$\sigma_{ij} = \frac{\sigma_i + \sigma_j}{2}$$

The electrostatic interactions require partial charges q_i assigned to each atom.

$$V_{Coulomb}(\mathrm{r},s) = V_{Coulomb}(\mathrm{r},q) = \sum_{i,j} \frac{1}{4\pi\varepsilon_0} \frac{q_i q_j}{r_{ij}}$$

In both the Lennard-Jones and the Coulomb potentials, r_{ij} denotes the distance between atoms i and j.

The force-field parameters are typically obtained by fitting a range of molecular (bonds, angles, etc.) and bulk (e.g. density, enthalpy of vaporization of liquid, or diffusion coefficient) properties obtained against data derived from either *ab-initio*

quantum mechanical calculations or experiment. The form of the potential energy function together with the parameters is called force-field.

The computational resources are not unlimited and, therefore, only a limited number of atoms can be simulated within reasonable time. Most simulations are restricted to tens of thousands of atoms. It is obvious that a system of even millions of atoms or molecules will be dominated by surface effects and will hardly reproduce properties of the bulk material (1 mole of material contains $6.022 \cdot 10^{23}$ particles!). The solution to this problem is introduction of the periodic boundary conditions (PBC) into the system. The system becomes pseudo-infinite. It is built of a primary simulation cell (a cube for example) and its replicated images (shifted by the integer number of the cube side length) that fill all space (Fig. 2.1). When energy and forces are calculated all atoms in the central box interact (ideally) with each other and with all images of the box at all distances. In practice, however, only limited number of couples is calculated for each atom. The reduction of the interactions can be achieve either via simple truncation beyond certain cut-off radius ($V = 0$ for $r > r_c$) or using "minimum image convention", where interaction with the nearest image of all particles is calculated.

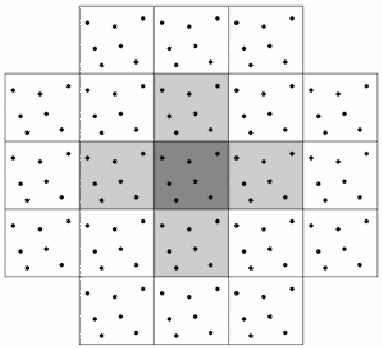

Figure 2.1. Periodic boundary conditions in MD simulations. The simulation box is replicated an infinite number of times and interactions between all atoms and their periodic images are calculated.

The bonded potentials are calculated directly and simply. The non-bonded Lennard-Jones potential decays very fast and is usually calculated only between atoms within a certain cut-off radius. The Coulomb potential has to be treated in a more sophisticated way, since electrostatic interactions are long-ranged and their contribution to the total energy and the forces between atoms at longer distances is not negligible. Therefore, many more images of the simulation box have to taken into account when electrostatic energies and forces are calculated. Moreover, convergence of the $V_{Coulomb}$ sum in direct space is very slow. This would result in unreasonably long computing times.

One way of accelerating the calculations of Coulomb sum is the Ewald summation method. With the help of a few mathematical transformations the sum is split into two sums. The first is done in real space and the second in reciprocal space (see the following subsection 2.2). Although this improves the convergence notably, the computational demand of the algorithm is still high. Faster is the reaction field method. In this case only electrostatic interactions of a selected atom with atoms within a certain cut-

off radius are considered. The space beyond the spherical cut-off is modeled as a dielectric medium of given permittivity that interacts with the selected atom in the center of the sphere. With this solution only few pair-wise interactions have to be calculated, which strongly speeds up the calculations. The method is, however limited to homogenous high-dielectric media. If there is an interface between two phases of very different permittivity the method may lead to artefacts.

Due to the fact that the metal is the conducting matter, it can be considered to have infinite dielectric permittivity. Thus, the interface between metal and organic matter, which is one of the subjects addressed in this thesis, should be preferably simulated using the Ewald summation approach (see subsection 2.2).

2.2. Simulations of metal surfaces: adaptation of the Ewald summation

The Ewald summation is a technique for efficiently summing the interaction between ions in the simulation box and all periodic images. The description of the method applied to the systems of point charges or dipole moments in three dimensional (3D) periodic boundary conditions can be found in the book of Allen and Tildesely[1]. The Ewald summation used for the current work has been modified in order to implement Finnis' model[7,8] of the electrostatic interaction of a metal slab with a point charge. Therefore, this subsection will focus mainly on those changes done.

For the system of N point charges in an orthogonal simulation box in 3D periodic boundary conditions, the electrostatic energy of the system looks as follows.

$$U_{Coulomb} = \frac{1}{2}\sum_{\mathrm{n}}{}^{!}\left(\sum_{i=1}^{N}\sum_{j=1}^{N}\frac{q_i q_j}{|\mathrm{r}_{ij}+\mathrm{n}|}\right) =$$

$$\frac{1}{2}\sum_{i=1}^{N}\sum_{j=1}^{N}\left(\sum_{|\mathrm{n}|=0}^{\infty}{}^{!}\, q_i q_j \frac{\mathrm{erfc}(\kappa|\mathrm{r}_{ij}+\mathrm{n}|)}{|\mathrm{r}_{ij}+\mathrm{n}|} + \frac{1}{\pi L_x L_y L_z}\sum_{k\neq 0} q_i q_j \frac{4\pi^2}{k^2}\exp\left(-\frac{k^2}{4\kappa^2}\right)\cos(\mathrm{k}\cdot\mathrm{r}_{ij})\right)$$

$$-\frac{\kappa}{\sqrt{\pi}}\sum_{i=1}^{N} q_i^2$$

where κ is the width of the cancelling Gaussian charge distribution around each of the point charges, L_x, L_y, L_z are the lengths of the simulation box, q_i are the values of the point charges, r_{ij} is the distance vector between charges i and j. The sum is performed over all lattice points, $\mathrm{n} = (n_x L_x, n_y L_y, n_z L_z)$ with n_x, n_y, n_z integers. The exclamation mark at the summation symbol ($\sum^{!}$) indicates that in the summation the term $i = j$ is omitted for $\mathrm{n} = 0$. The value of the width of the canceling distribution κ is usually chosen to be large enough in order to keep the real-space sum terms only for $|\mathrm{n}| = 0$. The terms for higher n ($\mathrm{n} \neq 0$) are small and can be neglected.

In the form given, the implementation of the Ewald sum is very slow. It can be speeded up via mathematical transformation of the reciprocal-space sum. Note that all prefactors are omitted for convenience and the $\cos(\mathrm{k}\cdot\mathrm{r}_{ij})$ term is replaced by the complex exponential $\exp(i\mathrm{k}\cdot\mathrm{r}_{ij})$, as for the final result only the real part is taken.

$$U_{reciprocal} = \sum_{i=1}^{N}\sum_{j=1}^{N}\sum_{k\neq 0} q_i q_j \frac{4\pi^2}{k^2}\exp\left(-\frac{k^2}{4\kappa^2}\right)\cos(\mathrm{k}\cdot\mathrm{r}_{ij})$$

$$\Rightarrow U_{reciprocal} = \sum_{i=1}^{N}\sum_{i=1}^{N}\sum_{k\neq 0} q_i q_j \frac{4\pi^2}{k^2}\exp\left(-\frac{k^2}{4\kappa^2}\right)\exp(i\mathrm{k}\cdot\mathrm{r}_{ij}) =$$

$$\sum_{k\neq 0}\frac{4\pi^2}{k^2}\sum_{i=1}^{N}\sum_{j=1}^{N} q_i q_j \exp\left(-\frac{k^2}{4\kappa^2}\right)\exp(i\mathrm{k}\cdot\mathrm{r}_{ij})$$

Using the fact that $\mathrm{r}_{ij} = \mathrm{r}_i - \mathrm{r}_j$ one can transform this sum into the following.

$$U_{reciprocal} = \sum_{k\neq 0}\frac{4\pi^2}{k^2}\sum_{i=1}^{N}\sum_{j=1}^{N} q_i q_j \exp\left(-\frac{k^2}{4\kappa^2}\right)\exp(i\mathrm{k}\cdot\mathrm{r}_i)\exp(-i\mathrm{k}\cdot\mathrm{r}_j) =$$

$$\sum_{k\neq 0}\frac{4\pi^2}{k^2}\left(\sum_{i=1}^{N} q_i \exp\left(-\frac{k^2}{4\kappa^2}\right)\exp(i\mathrm{k}\cdot\mathrm{r}_i)\right)\left(\sum_{i=1}^{N} q_i \exp\left(-\frac{k^2}{4\kappa^2}\right)\exp(-i\mathrm{k}\cdot\mathrm{r}_i)\right) =$$

$$\sum_{k\neq 0}\frac{4\pi^2}{k^2}\left|\sum_{i=1}^{N} q_i \exp\left(-\frac{k^2}{4\kappa^2}\right)\exp(i\mathrm{k}\cdot\mathrm{r}_i)\right|^2$$

Finally, the reciprocal sum can be expressed as

$$U_{reciprocal} = \sum_{k\neq 0}\frac{4\pi^2}{k^2} S(\mathrm{k})S^*(\mathrm{k}) = \sum_{k\neq 0}\frac{4\pi^2}{k^2}\left|S(\mathrm{k})\right|^2$$
$$S(\mathrm{k}) = \sum_{i=1}^{N} q_i \exp\left(-\frac{k^2}{4\kappa^2}\right)\exp(i\mathrm{k}\cdot\mathrm{r}_i) \quad ,$$

where the asterisk denotes the complex conjugate.

Furthermore, Finnis' model used in this work (Chapter 6) implies that there are both point charges and point dipole moments in the system at the same time. The descriptions available in the literature are for either point charges or point dipoles only. Therefore, there are additional computations necessary.

The forms of the electrostatic potential V of a point charge and a point dipole moment

$$V_q = \frac{q}{r}$$
$$V_{\mathrm{p}} = \frac{(\mathrm{p}\cdot\mathrm{r})}{r^3}$$

can be related to each other by replacing the term q in V_q by the $-\mathrm{p}\cdot\nabla$ operator, and then deriving V_{p}.

$$V_q(q=-\mathrm{p}\cdot\nabla) = -\mathrm{p}\cdot\nabla\frac{1}{r} = -\mathrm{p}\cdot\left(-\frac{\mathrm{r}}{r^3}\right) = \frac{(\mathrm{p}\cdot\mathrm{r})}{r^3} = V_{\mathrm{p}}$$

Therefore, using the same procedure and the energy of a point dipole in the field E ($U_{\mathrm{p}} = -(\mathrm{E}\cdot\mathrm{p})$) the expressions for the total energy U of a system with both point charges and point dipoles can be derived. Considering that every particle in the system comprises a point charge and a point dipole moment, the final expression for the energy of the system is

$$U = U_{real} + U_{reciprocal} + U_{self\ cancel}$$
$$U_{real} = \frac{1}{2}\sum_{i=1}^{N}\sum_{j=1}^{N}\left[q_i\left(\phi_{q,j}(\mathrm{r}_{ij}) + \phi_{\mathrm{p},j}(\mathrm{r}_{ij})\right) - \left(\mathrm{p}_i\cdot\left(\mathrm{e}_{q,j}(\mathrm{r}_{ij}) + \mathrm{e}_{\mathrm{p},j}(\mathrm{r}_{ij})\right)\right)\right]$$

where $\phi_{q,j}$ and $\phi_{\mathrm{p},j}$ are the potentials, $\mathrm{e}_{q,j}$ and $\mathrm{e}_{\mathrm{p},j}$ are the fields at the position of atom i due to charge and dipole of atom j

$$\phi_{q,j}(\mathrm{r}) = q\left[\sum_{|\mathrm{n}|=0}^{!}\frac{\mathrm{erfc}(\kappa|\mathrm{r}_{ij}+\mathrm{n}|)}{|\mathrm{r}_{ij}+\mathrm{n}|}\right]$$
$$\phi_{\mathrm{p},j}(\mathrm{r}) = -\mathrm{p}_j\nabla\phi_{q=1} = \left(\mathrm{p}_j\cdot\left[\sum_{|\mathrm{n}|=0}^{!}\left(\frac{\mathrm{erfc}(\kappa|\mathrm{r}_{ij}+\mathrm{n}|)}{|\mathrm{r}_{ij}+\mathrm{n}|^3} + \frac{2\kappa}{\sqrt{\pi}}\frac{\exp\left((\kappa|\mathrm{r}_{ij}+\mathrm{n}|)^2\right)}{|\mathrm{r}_{ij}+\mathrm{n}|^2}\right)(\mathrm{r}_{ij}+\mathrm{n})\right]\right)$$
$$\mathrm{e}_{q,j} = -\nabla\phi_{q,j} = q_j\sum_{|\mathrm{n}|=0}^{!}\left(\frac{\mathrm{erfc}(\kappa|\mathrm{r}_{ij}+\mathrm{n}|)}{|\mathrm{r}_{ij}+\mathrm{n}|^3} + \frac{2\kappa}{\sqrt{\pi}}\frac{\exp\left(-(\kappa|\mathrm{r}_{ij}+\mathrm{n}|)^2\right)}{|\mathrm{r}_{ij}+\mathrm{n}|^2}\right)(\mathrm{r}_{ij}+\mathrm{n})$$
$$\mathrm{e}_{\mathrm{p},j} = -\nabla\phi_{\mathrm{p},j} = \sum_{|\mathrm{n}|=0}^{!}\left[-\left(\frac{\mathrm{erfc}(\kappa|\mathrm{r}_{ij}+\mathrm{n}|)}{|\mathrm{r}_{ij}+\mathrm{n}|^3} + \frac{2\kappa}{\sqrt{\pi}}\frac{\exp\left((\kappa|\mathrm{r}_{ij}+\mathrm{n}|)^2\right)}{|\mathrm{r}_{ij}+\mathrm{n}|^2}\right)\mathrm{p}_j + \left(\frac{3\mathrm{erfc}(\kappa|\mathrm{r}_{ij}+\mathrm{n}|)}{|\mathrm{r}_{ij}+\mathrm{n}|^5} + \frac{2\kappa}{\sqrt{\pi}}\frac{\exp\left(-(\kappa|\mathrm{r}_{ij}+\mathrm{n}|)^2\right)}{|\mathrm{r}_{ij}+\mathrm{n}|^2}\left(2\kappa^2 + \frac{3}{|\mathrm{r}_{ij}+\mathrm{n}|^2}\right)\right)((\mathrm{r}_{ij}+\mathrm{n})\cdot\mathrm{p})(\mathrm{r}_{ij}+\mathrm{n})\right]$$

$$U_{reciprocal} = \frac{1}{2}\frac{1}{\pi L_x L_y L_z}\sum_{k\neq 0}\frac{4\pi^2}{k^2}\left[\left|S_q\right|^2 + S_{\mathrm{p}}S_q^* + S_q S_{\mathrm{p}}^* + \left|S_{\mathrm{p}}\right|^2\right]$$

$$S_q = \sum_{n=1}^{N} q_n \exp i(\mathrm{k}\cdot\mathrm{r}_n)$$

$$S_{\mathrm{p}} = \sum_{n=1}^{N} -i(\mathrm{k}\cdot\mathrm{p}_n)\exp i(\mathrm{k}\cdot\mathrm{r}_n)$$

Additionally, the correction term, which subtracts the artificial contribution to the total energy due to the interactions of the cancelling distribution with itself, must be accounted for.

$$U_{self\,cancel} = U_{q,sc} + U_{\mathrm{p},sc}$$

$$U_{q,sc} = -\frac{\kappa}{\sqrt{\pi}}\sum_{i=1}^{N} q_i^2$$

$$U_{\mathrm{p},sc} = -\frac{2\kappa^3}{3\sqrt{\pi}}\sum_{i=1}^{N} p_i^2$$

In our calculations of the electrostatic forces in the actual system with both point charges and point dipole moments the atoms that have non-zero dipole moments (metal surface) are fixed in space (Chapter 6). Therefore, only the forces acting on a number of selected point charges in this (belonging to the molecules above the surface) system needs to be derived.

$$\mathrm{f}_{q,i} = -\nabla_{q,\mathrm{r}_i} U$$

The subscript q indicates that only terms acting on q_i are taken. That is, the forces applied to dipole moments must be omitted.

Additionally, it is necessary to derive the coefficients of the C matrix (Chapter 6). These coefficients denote the value of the electrostatic potential and the field due to a point charge or a dipole moment.

$$V_q(\mathrm{r}) = qC^{Vq}(\mathrm{r})$$

$$V_{\mathrm{p}}(\mathrm{r}) = \mathrm{p}C^{V\mathrm{p}}(\mathrm{r})$$

$$\mathrm{E}_q(\mathrm{r}) = qC^{\mathrm{E}q}(\mathrm{r})$$

$$\mathrm{E}_{\mathrm{p}}(\mathrm{r}) = \mathrm{p}C^{\mathrm{E}\mathrm{p}}(\mathrm{r})$$

The coefficients can also be calculated using the Ewald sum. However, the reciprocal sum part can then not be optimized, as it has to be derived for either a single point charge or a dipole moment. Besides, the evaluation is performed at a position different from where the charge and the dipole moment are located. The coefficients C_{nm} that denote the

potential and field at site n due to a point charge at site m are calculated as in the following.

$$C_{nm}^{Vq} = C_{real} + C_{reciprocal}$$

$$C_{real} = \sum_{|\mathrm{n}|=0}{}^{!} \frac{\mathrm{erfc}\,(\kappa\,|\,\mathrm{r}_{nm}+\mathrm{n}\,|)}{|\,\mathrm{r}_{nm}+\mathrm{n}\,|}$$

$$C_{reciprocal} = \frac{4\pi}{L_x L_y L_z}\sum_{k\neq 0}\frac{\exp\left(i(\mathrm{k}\cdot\mathrm{r}_{nm})\right)\exp\left(-\dfrac{k^2}{4\kappa^2}\right)}{k^2}$$

$$C_{nm}^{\mathrm{E}q,\gamma} = C_{real}^{\gamma} + C_{reciprocal}^{\gamma}$$

$$C_{real}^{\gamma} = \sum_{|\mathrm{n}|=0}{}^{!}\left(\frac{\mathrm{erfc}\,(\kappa\,|\,\mathrm{r}_{nm}+\mathrm{n}\,|)}{|\,\mathrm{r}_{nm}+\mathrm{n}\,|^3} + \frac{2\kappa}{\sqrt{\pi}}\frac{\exp\left(-(\kappa\,|\,\mathrm{r}_{nm}+\mathrm{n}\,|^2)\right)}{|\,\mathrm{r}_{nm}+\mathrm{n}\,|^2}\right)(\mathrm{r}_{nm}+\mathrm{n})_{\gamma}$$

$$C_{reciprocal}^{\gamma} = -\frac{4\pi}{L_x L_y L_z}\sum_{k\neq 0}\frac{i\exp\left(i(\mathrm{k}\cdot\mathrm{r}_{nm})\right)\exp\left(-\dfrac{k^2}{4\kappa^2}\right)}{k^2}(\mathrm{k})_{\gamma}$$

where the index γ denotes the Cartesian component of the field vector (x, y, or z). The dipole moment counterparts are obtained via the formulas given below. In this case, the subscript γ describes the Cartesian component of the dipole moment whose contribution is considered (p_γ) and δ denotes the Cartesian component of the electrostatic field being calculated (E_δ). The symbol $\delta_{\gamma\delta}$ denotes the Kronecker delta.

$$C_{nm}^{V\mathrm{p},\gamma} = C_{real}^{\gamma} + C_{reciprocal}^{\gamma}$$

$$C_{real}^{\gamma} = \sum_{|\mathrm{n}|=0}{}^{!}\left(\frac{\mathrm{erfc}(\kappa\,|\,\mathrm{r}_{nm}+\mathrm{n}\,|)}{|\,\mathrm{r}_{nm}+\mathrm{n}\,|^3} + \frac{2\kappa}{\sqrt{\pi}}\frac{\exp\left(-(\kappa\,|\,\mathrm{r}_{nm}+\mathrm{n}\,|^2)\right)}{|\,\mathrm{r}_{nm}+\mathrm{n}\,|^2}\right)(\mathrm{r}_{nm}+\mathrm{n})_{\gamma}$$

$$C_{reciprocal}^{\gamma} = -\frac{4\pi}{L_x L_y L_z}\sum_{k\neq 0}\frac{i\exp\left(i(\mathrm{k}\cdot\mathrm{r}_{nm})\right)\exp\left(-\dfrac{k^2}{4\kappa^2}\right)}{k^2}(\mathrm{k})_{\gamma}$$

$$C_{nm}^{\mathrm{E}q,\gamma\delta} = C_{real}^{\gamma\delta} + C_{reciprocal}^{\gamma\delta}$$

$$C_{real}^{\gamma\delta} = \sum_{|\mathrm{n}|=0}{}^{!}\left[\begin{array}{l} -\left(\dfrac{\mathrm{erfc}(\kappa\,|\,\mathrm{r}_{nm}+\mathrm{n}\,|)}{|\,\mathrm{r}_{nm}+\mathrm{n}\,|^3} + \dfrac{2\kappa}{\sqrt{\pi}}\dfrac{\exp\left(-(\kappa\,|\,\mathrm{r}_{nm}+\mathrm{n}\,|^2)\right)}{|\,\mathrm{r}_{nm}+\mathrm{n}\,|^2}\right)\delta_{\gamma\delta} + \\ \left(\dfrac{3\mathrm{erfc}(\kappa\,|\,\mathrm{r}+\mathrm{n}\,|)}{|\,\mathrm{r}+\mathrm{n}\,|^5} + \dfrac{2\kappa}{\sqrt{\pi}}\dfrac{\exp\left(-(\kappa\,|\,\mathrm{r}+\mathrm{n}\,|)^2\right)}{|\,\mathrm{r}+\mathrm{n}\,|^2}\left(2\kappa^2 + \dfrac{3}{|\,\mathrm{r}+\mathrm{n}\,|^2}\right)\right)(\mathrm{r}+\mathrm{n})_{\gamma}(\mathrm{r}+\mathrm{n})_{\delta} \end{array}\right]$$

$$C_{reciprocal}^{\gamma\delta} = -\frac{4\pi}{L_x L_y L_z}\sum_{k\neq 0}\frac{i\exp\left(i(\mathrm{k}\cdot\mathrm{r}_{nm})\right)\exp\left(-\dfrac{k^2}{4\kappa^2}\right)}{k^2}(\mathrm{k})_{\gamma}(\mathrm{k})_{\delta}$$

The set of these equations is used for the simulations of the interface between platinum(111) and liquid isopropanol (Chapter 6).

2.3. References

(1) Allen, M. P.; Tildesley, D. J. *Computer Simulation of Liquids*; Oxford University Press: Oxford, 1987.

(2) Frenkel, D.; Smit, B. *Understanding Molecular Simulation: From Algorithms to Applications*, 2nd ed.; Academic Press: San Diego, 2002.

(3) Glaettli, A. Computer simulation of biomolecular systems: From the formulation of models for water, to the interpretation of experiment, to the investigation of polypeptide folding and membrane protein dynamcs., Swiss Federal Institute of Technology, 2004.

(4) Müller-Plathe, F. *Comput. Phys. Commun.* 1990, *61*, 285.

(5) Müller-Plathe, F. *Comput. Phys. Commun.* 1993, *78*, 77.

(6) Tarmyshov, K. B.; Müller-Plathe, F. *J. Chem Inf. Model.* 2005, *45*, 1943.

(7) Finnis, M. W. *Surf. Sci.* 1991, *241*, 61.

(8) Finnis, M. W.; Kaschner, R.; Kruse, C.; Furthmuller, J.; Scheffler, M. *J. Phys.-Condes. Matter* 1995, *7*, 2001.

3. Applications

3.1. Molecular recognition

Supramolecular chemistry can be defined as "chemistry beyond the molecule", based on the organized entities of higher complexity that result from the association of two or more chemical species held together by intermolecular forces. The partners of supramolecular species are named "molecular receptor/container" and "substrate/guest", the guest being usually the smaller component whose binding is being sought (molecular recognition).

Molecular interactions build the basis of highly specific recognition, reaction, transport, regulation, etc. processes that take place in biology, such as guest binding to a receptor protein, enzymatic reactions, assembling of protein-protein complexes, immunological antigen-antibody association, intermolecular reading, translation, and transcription of the genetic code, signal induction by neurotransmitters, and cellular recognition. The design of artificial molecular receptors of high selectivity and efficiency requires the correct manipulation of the non-covalent, intermolecular forces (van der Waals, electrostatic interactions, hydrogen bonding, etc.) within a certain molecular architecture.

Chemistry is not limited to systems found in nature, but is free to create novel species and to invent processes. Understanding molecular recognition requires a model of atomic resolution. In the field of molecular recognition, simulations and experiment collaborate to provide mutual support. While experimentalists are restrained to deal only with the systems that exist physically, simulations can be utilized to model a molecular species that does not exist in the nature. In pharmaceutical research, for instance, unphysical substrates (guests) are used in simulations. It supplements experimental work and helps to search faster for possible guests that can be bound by proteins[1]. The results of binding of unphysical compounds can provide hints how possible real compounds should look like to be very likely to bind. Simulations can also be used to predict binding constants or to study precise binding mechanism and main encapsulation driving forces.

There are some synthetic cyclic containers that are widely used in industry and research. Among them are cyclodextrins[2-7] (e.g. receptor[2,6], drug-delivery[7], enzyme models[5]), calixarenes[8-12] (drug delivery[9], extraction of uranium[12]), crown ethers[13-16] (cation selectivity[13,15,16]). These are just few examples of applications where these receptors can be used. The list of applications is growing still.

A novel class of cyclic receptors that has been investigated intensively in the last years is cucurbit[*n*]uril (CB)[17,18]. It has a capability to capture and release of guests in salt solutions in response to pH[19,20], change binding constant in response to salt concentration[21], or to change stochiometry of complex via redox reaction[22]. It is also possible to change and improve fluorescence properties of encapsulated compounds[23-25]. Via molecular dynamics simulations we observed the behaviour of metal cations associating with CB[6] and speculate about the effect of different cations on the

behaviour of the guest in the receptor. Chapter 5 is devoted to CB[6] in aqueous solutions of different salts and shows that the idea based on the experimental data and that assumes cations working as "lids" at the portals of CB[6] can not be confirmed in its current form.

3.2. Polymer/solid interfaces

An important area of applications is the interfaces of polymers with other materials, particularly with solid surfaces. Cars, planes, and other machines, furniture, some consumer electronics[26], walls of buildings are coated with polymers for colour effect (painting) or for improvement of corrosion resistance[27-30] (coating); some polymers can be used for adhesive purposes[31-34]; the properties of the polymer/solid interfaces are also crucial for production of (nano)composites[35-37] and filled polymer materials. These are just few known applications of polymer/solid interfaces, where the features of interactions between solid surface and polymer molecules are crucial.

Simulations allow scientists to get an insight into what is going on immediately at the interface and a little further from it[38-43]. One can estimate such properties as density profile, diffusion coefficient, ordering/structure to explain experimentally obtained results[44-47]. Molecular dynamics simulations also allow scientists to find out the influence of different types of interactions between surface and adsorbate on the properties of the interface. By simply switching them off and comparing the properties of interest one can say how these important interactions are. This type of theoretical experiment can also give an idea of which types of interactions must be accounted for in simulations and which are optional for this particular feature of the system. In a similar spirit, Chapter 6 demonstrates, for example, that accounting for electrostatic interactions between liquid isopropanol and platinum surface does not drastically change the properties of the interface, although the calculation of these interactions requires a lot of computer resources. Short-range interactions (chemisorption), on the other hand, are crucial for description of properties as density, ordering, and diffusion.

3.3. References

(1) Oostenbrink, C.; van Gunsteren, W. F. *Proceedings of the National Academy of Sciences of the United States of America* 2005, *102*, 6750.
(2) Georg, H. C.; Coutinho, K.; Canuto, S. *Chem. Phys. Lett.* 2005, *413*, 16.
(3) Ivanov, P. M.; Jaime, C. *J. Phys. Chem. B* 2004, *108*, 6261.
(4) Mohanambe, L.; Vasudevan, S. *Langmuir* 2005, *21*, 10735.
(5) Rizzarelli, E.; Vecchio, G. *Coord. Chem. Rev.* 1999, *188*, 343.
(6) Yu, Y. M.; Chipot, C.; Cai, W. S.; Shao, X. G. *J. Phys. Chem. B* 2006, *110*, 6372.
(7) Uekama, K.; Hirayama, F.; Arima, H. *J. Incl. Phenom. Macrocycl. Chem.* 2006, *56*, 3.
(8) Haino, T.; Yanase, M.; Fukunaga, C.; Fukazawa, Y. *Tetrahedron* 2006, *62*, 2025.
(9) Da Silva, E.; Lazar, A. N.; Coleman, A. W. *J. Drug Deliv. Sci. Technol.* 2004, *14*, 3.
(10) LaraOchoa, F.; Cogordan, J. A.; SilaghiDumitrescu, I. *Fullerene Sci. Technol.* 1996, *4*, 887.
(11) Tokunaga, Y.; Sakon, H.; Kanefusa, H.; Shimomura, Y.; Suzuki, K. *Arkivoc* 2003, 135.
(12) Boulet, B.; Bouvier-Capely, C.; Cossonnet, C.; Cote, G. *Solvent Extr. Ion Exch.* 2006, *24*, 319.
(13) Lamare, V.; Haubertin, D.; Golebiowski, J.; Dozol, J. F. *J. Chem. Soc. Perkin Trans. 2* 2001, 121.
(14) Bokare, A. D.; Patnaik, A. *J. Phys. Chem. A* 2005, *109*, 1269.
(15) Troxler, L.; Wipff, G. *J. Am. Chem. Soc.* 1994, *116*, 1468.
(16) Vayssiere, P.; Chaumont, A.; Wipff, G. *Phys. Chem. Chem. Phys.* 2005, *7*, 124.
(17) Lee, J. W.; Samal, S.; Selvapalam, N.; Kim, H. J.; Kim, K. *Accounts Chem. Res.* 2003, *36*, 621.
(18) Lagona, J.; Mukhopadhyay, P.; Chakrabarti, S.; Isaacs, L. *Angew. Chem. Int. Edit.* 2005, *44*, 4844.
(19) Jeon, Y. M.; Kim, H.; Whang, D.; Kim, K. *J. Am. Chem. Soc.* 1996, *118*, 9790.
(20) Marquez, C.; Nau, W. M. *Angew. Chem. Int. Edit.* 2001, *40*, 3155.
(21) Marquez, C.; Hudgins, R. R.; Nau, W. M. *J. Am. Chem. Soc.* 2004, *126*, 5806.
(22) Jeon, W. S.; Kim, H. J.; Lee, C.; Kim, K. *Chem. Commun.* 2002, 1828.
(23) Mohanty, J.; Bhasikuttan, A. C.; Nau, W. M.; Pal, H. *J. Phys. Chem. B* 2006, *110*, 5132.
(24) Koner, L. A.; Nau, W. M. *Supramol. Chem.* 2006, *In press*.
(25) Nau, W. M.; Mohanty, J. *Int. J. Photoenergy* 2005, *7*, 133.
(26) Duan, J.; Wan, K. T.; Chian, K. S. *Thin Solid Films* 2003, *424*, 120.
(27) Beck, F.; Michaelis, R.; Schloten, F.; Zinger, B. *Electrochim. Acta* 1994, *39*, 229.
(28) Yagan, A.; Pekmez, N. O.; Yildiz, A. *Prog. Org. Coat.* 2006, *57*, 78.
(29) Schauer, T.; Joos, A.; Dulog, L.; Eisenbach, C. D. *Prog. Org. Coat.* 1998, *33*, 20.
(30) Zhu, H.; Zhong, L.; Xiao, S. H.; Gan, F. X. *Electrochim. Acta* 2004, *49*, 5161.
(31) Chantaratcharoen, A.; Sirisinha, C.; Amornsakchai, T.; Bualek-Limcharoen, S.; Meesiri, W. *J. Appl. Polym. Sci.* 1999, *74*, 2414.

(32) Creton, C.; Lakrout, H. *J. Polym. Sci., Part B: Polym. Phys.* 2000, *38*, 965.
(33) Ghatak, A.; Mahadevan, L.; Chaudhury, M. K. *Langmuir* 2005, *21*, 1277.
(34) Raegen, A. N.; Dalnoki-Veress, K.; Wan, K. T.; Jones, R. A. L. *Eur. Phys. J. E* 2006, *19*, 453.
(35) Bruzaud, S.; Grohens, Y.; Ilinca, S.; Carpentier, J. F. *Macromol. Mater. Eng.* 2005, *290*, 1106.
(36) de Oliveira, H. P.; Andrade, C. A. S.; de Melo, C. P. *Synth. Met.* 2005, *155*, 631.
(37) Fritzsche, W.; Porwol, H.; Wiegand, A.; Bornmann, S.; Kohler, J. M. *Nanostruct. Mater.* 1998, *10*, 89.
(38) Pal, S.; Weiss, H.; Keller, H.; Müller-Plathe, F. *Langmuir* 2005, *21*, 3699.
(39) Jhon, Y. I.; Kim, H. G.; Jhon, M. S. *J. Colloid Interface Sci.* 2003, *260*, 9.
(40) Raghavan, K.; Foster, K.; Motakabbir, K.; Berkowitz, M. *J. Chem. Phys.* 1991, *94*, 2110.
(41) Schravendijk, P.; van der Vegt, N.; Delle Site, L.; Kremer, K. *ChemPhysChem* 2005, *6*, 1866.
(42) Abrams, C. F.; Delle Site, L.; Kremer, K. *Phys. Rev. E* 2003, *67*.
(43) Roy, S.; Jin, R. Y.; Chaudhary, V.; Hase, W. L. *Comput. Phys. Commun.* 2000, *128*, 210.
(44) Glebov, A.; Graham, A. P.; Menzel, A.; Toennies, J. P. *J. Chem. Phys.* 1997, *106*, 9382.
(45) Haq, S.; Harnett, J.; Hodgson, A. *Surf. Sci.* 2002, *505*, 171.
(46) Jacob, T.; Goddard, W. A. *J. Am. Chem.* 2004, *126*, 9360.
(47) Jacob, T.; Muller, R. P.; Goddard, W. A. *J. Phys. Chem. B* 2003, *107*, 9465.